Differentiation of Microbial Species and Strains in Coculture Biofilms by Multivariate Analysis of Laser Desorption Postionization Mass Spectra

Chhavi Bhardwaj[1], Yang Cui[1], Theresa Hofstetter[2], Suet Yi Liu[2], Hans C. Bernstein[3], Ross P. Carlson[3], Musahid Ahmed[2] and Luke Hanley[1,*]

[1]Department of Chemistry, University of Illinois at Chicago, Chicago, IL 60607-7061

[2]Chemical Sciences Division, Lawrence Berkeley National Laboratory, Berkeley, CA 94720

[3]Center for Biofilm Engineering, Montana State University, Bozeman, MT 59717

Abstract

7.87 to 10.5 eV vacuum ultraviolet (VUV) photon energies were used in laser desorption postionization mass spectrometry (LDPI-MS) to analyze biofilms comprised of binary cultures of interacting microorganisms. The effect of photon energy was examined using both tunable synchrotron and laser sources of VUV radiation. Principal components analysis (PCA) was applied to the MS data to differentiate species in *Escherichia coli-Saccharomyces cerevisiae* coculture biofilms. PCA of LDPI-MS also differentiated individual *E. coli* strains in a biofilm comprised of two interacting gene deletion strains, even though these strains differed from the wild type K-12 strain by no more than four gene deletions each out of approximately 2000 genes. PCA treatment of 7.87 eV LDPI-MS data separated the *E. coli* strains into three distinct groups two "pure" groups and a mixed region. Furthermore, the "pure" regions of the *E. coli* cocultures showed greater variance by PCA when analyzed by 7.87 eV photon energies than by 10.5 eV radiation. Comparison of the 7.87 and 10.5 eV data is consistent with the expectation that the lower photon energy selects a subset of low ionization energy analytes while 10.5 eV is more inclusive, detecting a wider range of analytes. These two VUV photon energies therefore give different spreads via PCA and their respective use in LDPI-MS constitute an additional experimental parameter to differentiate strains and species.

*Corresponding author, email: LHanley@uic.edu

I. Introduction

Many microorganisms live within complex surface associated communities known as biofilms.[1] Biofilms can be comprised of monocultures or more commonly, exist as consortia of multiple interacting species.[2,3] Consortial biofilms can exhibit complex interspecies relationships and dependencies that are the subject of many ongoing investigations.[4,5] Controlling problematic medical or beneficial environmental multispecies biofilms is challenging due to limited knowledge of the critical interactions occurring between the microorganisms organized within microscale structures. Spatially differentiating strains or species in a mixed culture biofilm can provide useful information, such as localization of available metabolic potential as well as provide insight into the competitive nature of the metabolic interactions.[6,7]

Escherichia coli and *Saccharomyces cerevisiae* are arguably the best-studied prokaryotic and eukaryotic microorganisms, respectively, and serve as ideal model systems for developing techniques to examine biofilm interactions. The current study employs two distinct binary cocultures designed to mimic a naturally occurring producer-consumer ecological motif which revolves around exchanges of metabolites between microorganisms.[5] Both cocultures have a glucose-oxidizing producer member, either an *E. coli* deletion mutant[8] or the baker's yeast *S. cerevisiae*, which cross feed metabolic byproducts such as acetate or ethanol to a glucose-negative *E. coli* consumer strain which acts as the system's scavenger.

Multivariate analysis aids the analysis of complex and multi-component systems and is commonly used for processing large data sets from the chemical analysis of biofilms and other intact biological samples. Principal component analysis (PCA) is the most commonly used and widely reported of the various multivariate analysis methods. PCA decomposes data with correlated measurements into a new set of uncorrelated (i.e., orthogonal) variables called principal components.[9] PCA is ideal for dealing with large data sets such as mass spectra,[10-12]

because it reduces their size with a minimal loss of information. For these reasons, PCA is often used for classification and/or grouping of experimental results to extract useful information. Several studies have differentiated strains of microorganisms by PCA of matrix assisted laser desorption ionization mass spectra (MALDI-MS)[13,14] and secondary ion mass spectra (SIMS).[12,15]

Both with and without PCA, SIMS and MALDI-MS have been widely used for MS imaging of biofilms and other intact biological samples.[16-20] SIMS has the advantage of high spatial resolution. However, molecular information for many species is often lost to fragmentation in SIMS, which readily detects low mass (m/z <300) and atomic ions. MALDI-MS is less chemically destructive than SIMS and is often used to detect molecular ions of species up to several kDa mass. However, MALDI-MS has lower spatial resolution than SIMS and requires extensive sample preparation such as the addition of matrix, which can obscure species in the low mass range. Both SIMS and MALDI-MS typically require thin, electrically conductive samples. Finally, ion suppression and local fluctuations in ionization efficiency can complicate quantification in these and other methods in MS imaging.[20]

Some of the limitations of SIMS and MALDI-MS for the analysis of biofilms and other biological samples can be overcome using laser desorption postionization mass spectrometry (LDPI-MS), which uses vacuum ultraviolet (VUV) radiation to induce a relatively 'soft' single photon ionization of laser desorbed neutrals.[21,22] LDPI-MS, also referred to as two laser mass spectrometry (L2MS),[23] does not require the addition of a matrix compound to enhance desorption. LDPI-MS is not sensitive to ion suppression since it detects desorbed neutrals and shows some advantages for quantification.[24] Furthermore, LDPI-MS can readily analyze thick, electrically insulating samples.[25]

The ability of LDPI-MS to detect intact parent ions of molecular species depends upon the extent of energy transfer during the separate laser desorption and single photon ionization steps. Prior LDPI-MS work with 8.0 - 12.5 eV VUV photon energies showed that higher photon energies improve sensitivity, producing intense molecular ion signal, but at the expense of enhanced formation of fragment ions and background gas ions.[26,27] Because the 10.5 eV photon energy appeared to provide the optimal balance between improved sensitivity and minimal fragmentation, a new design for a laboratory source of 10.5 eV radiation was recently developed.[25]

The present study utilized 7.87 to 10.5 eV VUV photon energies in LDPI-MS to analyze biofilms comprised of binary cultures of interacting microorganisms. The effect of photon energy was examined using both tunable synchrotron and laser sources of VUV radiation. PCA was applied to the MS data to differentiate species in *E. coli-S. cerevisiae* biofilms and to differentiate individual *E. coli* strains in a biofilm comprised of two interacting gene deletion strains. Clear spatial separation of both these two species as well as different *E. coli* strains, based on their distinct metabolic states, was demonstrated by PCA of LDPI-MS of intact biofilms.

II. Experimental Details

A. Biofilm growth and sample preparation. Biofilm culturing conditions were identical to those reported previously.[25] The two *E. coli* K-12 deletion mutant strains (403G100-ΔptsGΔptsMΔglkΔgcd expressing the reporter protein ds-tomato and 307G100-ΔaceAΔldhAΔfrdA expressing reporter protein citrine, are termed here the tomato and citrine strain, respectively) and their growth conditions were described previously.[8] The yeast, *S.*

cerevisiae, was grown using a similar protocol. The term monoculture refers to a biofilm sample with only one species or strain. The term coculture refers to a binary culture of two genetically distinct microorganisms that have been grown together on the same substrate. The coculture biofilms grown here were inoculated initially a few mm apart by two monocultures, then allowed to grow towards each other until they visually overlapped. LDPI-MS analysis of coculture samples was performed on three distinct regions: two spots comprised predominantly of one type of microbe ("pure" region at the outer edges of the coculture sample) and at the center of the sample where the two species visually overlapped ("mixed" region).

Biofilms were grown on insulating polycarbonate membranes, the membranes were then adhered to a stainless steel plate with copper tape for introduction into vacuum for MS analysis. Biofilms were also blotted onto stainless steel plates: the blots were then introduced into vacuum.

B. LDPI-MS instrumentation. LDPI-MS analysis was carried out on customized instruments utilizing either quasi-continuous synchrotron or pulsed laser VUV postionization sources. Details of the synchrotron LDPI-MS instrument have been reported previously and can be found elsewhere.[26-29] The synchrotron LDPI-MS is located on the Chemical Dynamics Beamline at the Advanced Light Source (Lawrence Berkeley National Laboratory, Berkeley, CA).[30] It is a commercial SIMS instrument (TOF.SIMS 5, ION-TOF Inc., Munster, Germany) which was modified by the addition of a 349 nm Nd:YLF pulsed desorption laser (Spectra-Physics Explorer, Newport Corporation, Irvine, CA). This laser was operated at 2500 Hz repetition rate with a spot size of ~30 μm diameter and laser desorption peak power density of 1 to 10 MW/cm^2. Tunable VUV synchrotron radiation in the range of 7.87 - 10.5 eV photon energy was used for the ionization of desorbed neutrals.

The laser LDPI-MS at the University of Illinois at Chicago was also described previously.[22,25] A 349 nm Nd:YLF laser (Spectra-Physics Explorer) was used for desorption at 10 or 100 Hz repetition rate which depended on the VUV ionization laser. The desorption laser beam was used at peak power density of ~300 MW/cm^2 with a ~50 μm diameter beam on the biofilm. Laser postionization was carried out at two fixed photon energies: 7.87 and 10.5 eV. A 157.6 nm fluorine laser (Optex Pro, Lambda Physik, Ft Lauderdale, FL) operating at 100 Hz was used for 7.87 eV postionization with a cross sectional area of 2 × 1 mm^2 and an energy of ~100 μJ/pulse. 10.5 eV laser postionization was performed with a 118 nm beam generated by tripling the third harmonic of a Nd:YAG laser (355 nm, ~20 mJ, 5 ns, Tempest, New Wave Research, Fremont, CA) in a Xe gas cell at 6.5 Torr pressure, as described previously.[25] The resulting photoions were pulse extracted and analyzed using a reflectron TOF which is similar to that described previously.[25] Software used for data acquisition was partially described elsewhere with respect to its use on a different instrument.[31]

The sample stage on the synchrotron LDPI-MS was moved to analyze a ~3 mm^2 area for each biofilm sample with 10 laser shots per spot before moving to an fresh spot for repeated analysis. ~1.2 × 10^5 laser shots were used for collecting each displayed synchrotron mass spectrum. The laser LDPI-MS utilized a sample stage that was continuously moving at a speed of 0.05 mm/s while the desorption laser scanned over the sample for a total area of analysis of 1 mm^2. Mass spectra were averaged over the entire analyzed area. ~4 × 10^4 laser shots were used to collect each laser LDPI mass spectrum presented here.

C. Data acquisition and analysis. Reported m/z peaks were observed reproducibly for at least three replicate mass spectra. The peaks listed in Table 1 were chosen by careful visual examination. A custom program was designed in house for peak picking directly from the raw

data after applying binning and baseline correction. This program selected integer m/z values of peak centroids based on a defined peak width. All spectra were normalized before peak picking in order to remove any variance not due to actual chemical difference between samples.

A nonlinear iterative partial least squares algorithm from MATLAB (The MathWorks Inc., Natick, MA) was used to perform PCA.[32,33] The mass range chosen for all the reported PCA was m/z 50 - 700. An n × p data matrix was obtained where n was the experiment trials and p represented ion intensities with corresponding m/z values. LDPI-MS data were preprocessed by mean centering and scaling of the columns of the original data matrix. Each data set used in the analysis was replicated at least three times and a minimum of 15 spectra of each microbe type was used to compose the original data matrix.

III. Results

A. VUV Photon Energy Dependence on Monoculture Biofilms. Blots of yeast monoculture biofilms were analyzed by synchrotron LDPI-MS using 7.87, 8.5, 9.5 and 10.5 eV VUV photon energies with the results shown in Figure 1. The synchrotron LDPI-MS of yeast monocultures showed that increasing photon energy resulted in more peaks in the mass spectra and higher overall signal intensity. Fragmentation increased significantly at photon energies up to ~15 eV (data not shown). Overall, 10.5 eV photon energy displayed an optimal balance between sensitivity and fragmentation, in agreement with prior experiments.[26,27,34] Similar conclusions were reached from 7.87 - 10.5 eV synchrotron LDPI-MS of *E. coli* (tomato strain) monoculture blots (full mass spectra shown in Supporting Information).

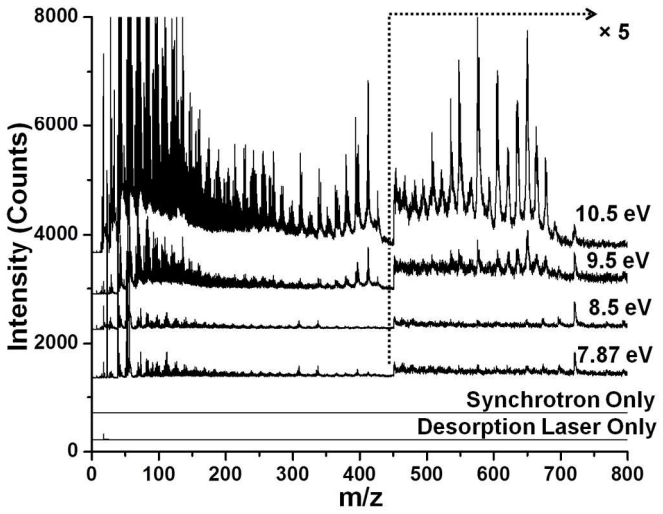

Figure 1: 7.87 - 10.5 eV synchrotron laser desorption postionization mass spectra (LDPI-MS) of blotted yeast monoculture biofilms. The bottom two traces show the controls performed with only synchrotron photoionization or desorption laser.

The mass spectral peaks observed for *E. coli* and yeast monocultures were tabulated with the VUV photon energies at which they were first observed by synchrotron LDPI-MS. Table 1 shows the list of peaks observed at different photon energies: peaks first appearing at 7.87 eV are shown in the left column of Table 1 while additional peaks appearing at 9.5 and 10.5 eV photon energies are listed in the middle and right column, respectively. Peaks observed at lower photon energies always appeared at higher photon energies as well, albeit at higher intensities. However, a separate column is not shown for 8.5 eV photon energy, since no new peaks were observed visually beyond those already present at 7.87 eV.

Prior synchrotron LDPI-MS studies [26,27] led to the recent development of a refined laboratory VUV photoionization source that operates at 10.5 eV[25] to complement the 7.87 eV fluorine excimer laser source.[22] These two laboratory laser VUV sources were used to collect 7.87 and 10.5 eV laser LDPI-MS data from *E. coli* and yeast monocultures. 10.5 eV laser LDPI-MS data for blotted monoculture biofilms (yeast or *E. coli*) was collected and compared with the similar spectra collected by 10.5 eV synchrotron LDPI-MS (see Supporting Information). The

synchrotron LDPI-MS data of the blotted samples showed overall higher S/N compared to that from laser LDPI-MS.

Table 1: List of mass peaks (units of m/z) first observed at 7.87, 9.5, and 10.5 eV photon energies by synchrotron LDPI-MS of blots of *E. coli* bacteria and *S. cerevisiae* yeast monocultures.

Species	7.87 eV (m/z)	9.5 eV (m/z)	10.5 eV (m/z)
***Escherichia coli* (Bacteria)**	39-45, 53-58, 65-75, 77-87	35	
	95-105, 108-115, 120-130, 135-145, 157, 159, 165, 175, 180, 181,197	153	
	267	212-216, 240, 251	228, 256
	366	315, 326, 338, 371	
	590	550, 565, 578	
	605, 625, 635		665
	732, 745, 763, 780, 793	730, 750, 775	
***Saccharomyces cerevisiae* (Yeast)**	38-45, 53-60, 67-75, 82-88		32, 34, 48
	90-105, 105-115, 135-143	145-150	128, 156, 168-172, 184-194, 198-205
	235-245, 250-260, 264-270, 276-284	213-216, 227-230, 272	
	397	394, 398, 400	395, 396
	413	412, 415, 426	494
	576	508, 536, 564-568, 592-596	510-514, 522, 552
	696-700		
	720-724		
	816-818, 840-845		

The data traces labeled “Desorption Laser Only” and “Synchrotron Only” in Figure 1 demonstrate the absence of any background signal arising from direct ionization via the desorption laser or VUV postionization of background or sublimed gaseous neutrals,

respectively. Prior control experiments with the 10.5 eV laser LDPI-MS established the presence of single photon ionization and ruled out both direct ions from laser desorption and photoelectron ionization effects due to the residual 355 nm beam used to generate VUV radiation.[25] Photoelectron ionization was previously ruled out in the synchrotron LDPI-MS.[27] The similarity of the spectra by 7.87 eV synchrotron and laser LDPI-MS ruled out photoelectron ionization in the latter case.

B. Analysis of intact biofilms vs. blotted samples. It is convenient technically to grow biofilms on polymer membranes, but these insulating membranes can complicate analysis by MS imaging strategies. Membrane biofilm analyses were attempted on the synchrotron LDPI-MS instrument, but reproducible MS signal was elusive due to what appeared to be excessive sample charging of these electrically insulating membrane. However, intact membrane biofilms could be analyzed directly in vacuum by laser LDPI-MS, as discussed below.

Figure 2 shows 10.5 eV laser LDPI mass spectra of blotted and intact biofilm samples from yeast monocultures. There was ~8× higher S/N for the intact membrane samples compared to the blotted biofilms. Although the same peaks were observed for both samples, overall peak intensity was higher for membrane samples. Additionally, peaks at m/z 600 - 700 were not discernible in the blotted sample due to low S/N.

Direct comparison was also made for membrane biofilms analyzed with laser LDPI-MS vs. blotted biofilms analyzed with synchrotron LDPI-MS: the different spectra showed similar peaks, albeit with differences in S/N and absolute signal intensity. The synchrotron MS data showed more peaks in the low mass (< m/z 300) region.

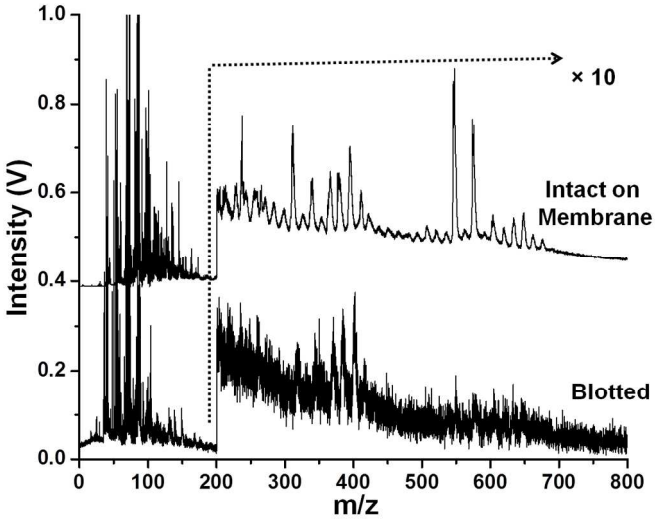

Figure 2: 10.5 eV laser LDPI-MS of yeast monoculture biofilms using two different sample preparation techniques. Spectra are normalized.

Intact membrane biofilms were not observed to delaminate in vacuum and maintained their structural integrity. However, the blotted biofilms occasionally suffered from delamination in vacuum which adversely impacted the synchrotron LDPI-MS. The continuous synchrotron radiation readily ablated delaminating pieces since the VUV beam passed very close to the top of the sample, leading to signal spikes near m/z 270 in the MS. Ablation signal was not observed in laser LDPI-MS since the pulsed VUV beam passed farther above the sample, missing the delaminated pieces of biofilm. In any case, ablation would occur to a lesser extent by the pulsed VUV laser beam whose duty cycle was 10^{-6} at 7.87 eV and 10^{-7} at 10.5 eV (vs. near unity for the quasi-continuous synchrotron radiation).

C. Coculture multispecies biofilms. 10.5 eV synchrotron LDPI-MS were recorded at three distinct regions of blotted *E. coli* and yeast coculture biofilms (see Supporting Information). The "pure" *E. coli* and yeast regions of the biofilms generated spectra that generally appeared similar to those from the corresponding monocultures. However, synchrotron LDPI-MS of the mixed region of the coculture biofilms tended to vary from one sample to the

next. This variability might have resulted from the limitation of sample preparation: the clear boundaries of the microbial species were not visually apparent in the blotted samples, making it difficult to assign a given region to a specific species. Additionally, synchrotron LDPI-MS were acquired with the desorption laser scanning over a relatively large, ~3 mm^2 area for each region, increasing the possibility of overlap of the different regions.

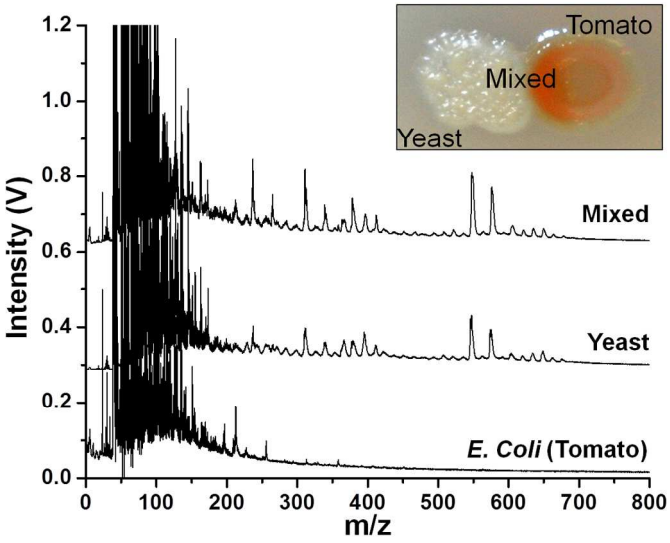

Figure 3: 10.5 eV laser LDPI-MS of coculture *E. coli* (tomato strain) and yeast multispecies membrane biofilm. "Mixed" indicates the region of overlap between the two species while other spectra correspond to "pure" regions of biofilms, as labeled in the inset photo of a typical coculture biofilm.

By contrast, the laser LDPI-MS allowed analysis of a ~1 mm^2 area of an intact membrane biofilm with relatively high S/N. Therefore, both coculture *E. coli* and yeast biofilms were studied using both the 7.87 and 10.5 eV laser photoionization sources, with Figure 3 showing the latter result. The trace labeled "Mixed" in Figure 3 refers to the region where the two species overlap. The "pure" regions of *E. coli* and yeast could be readily distinguished by visual examination of the intact membrane biofilms and the mass spectra at both photon energies appeared similar to those of their respective monocultures. The mass spectra for the mixed region showed peaks from both of the species. 10.5 eV laser LDPI-MS showed more peaks in the

high mass region (m/z > 400) compared to 7.87 eV data, indicating more molecular species were ionized at the higher photon energy (see data in Supporting Information and compare with Table 1).

D. PCA of LDPI-MS for strain and species differentiation. The results above demonstrated the capability of LDPI-MS to study monoculture biofilms as well as multistrain and multispecies coculture biofilms (see also Supporting Information). PCA was performed on the laser LDPI-MS data from coculture biofilms to demonstrate an ability to differentiate species and strains in different regions of the biofilm. The approach was optimized by first applying PCA to the clearly distinct MS data of *E. coli* and yeast in a coculture biofilm sample (see Supporting Information). Given that these two microbes showed obvious mass spectral differences for the "pure" regions of each species, it is not surprising that applying PCA to the data also readily distinguished the two species.

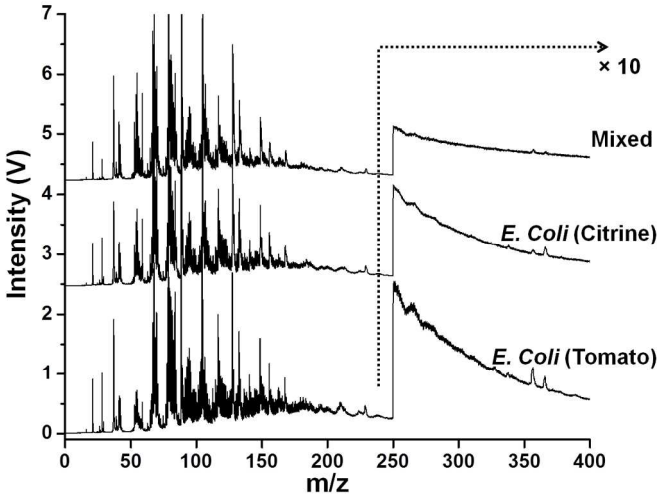

Figure 4: 7.87 eV laser LDPI-MS of coculture *E. coli* (tomato and citrine) multistrain membrane biofilm. "Mixed" indicates the region of overlap between the two strains.

The optimized PCA protocol was then applied to a more challenging system wherein a multistrain *E. coli* membrane biofilm was examined. Both 7.87 eV and 10.5 eV laser LDPI-MS

data of the genetically similar tomato and citrine *E. coli* strains were collected, with the former shown in Figure 4 and the latter reported previously.[25] Figures 5a shows a plot of principal component 1 vs. principal component 2 for the 7.87 eV laser LDPI-MS data. While the mass spectra of the two strains in coculture samples showed only minor visual differences in the peak pattern, PCA treatment of the "pure" regions of the sample resulted in grouping the two strains separately. Furthermore, the mixed region was clearly distinguished from the two "pure" regions suggesting metabolic interactions resulted in altered physiologies. Figures 5b is a scree plot[9] which shows the variance of the entire data set with respect to the principal components. The scree plot indicates that ~80% of the variance for the data is represented by its first two principal components. Similarly, PCA was performed on the corresponding 10.5 eV MS data (see Supporting Information): it also distinguished the two "pure" regions of the biofilm, albeit with most variance along the first principal component.

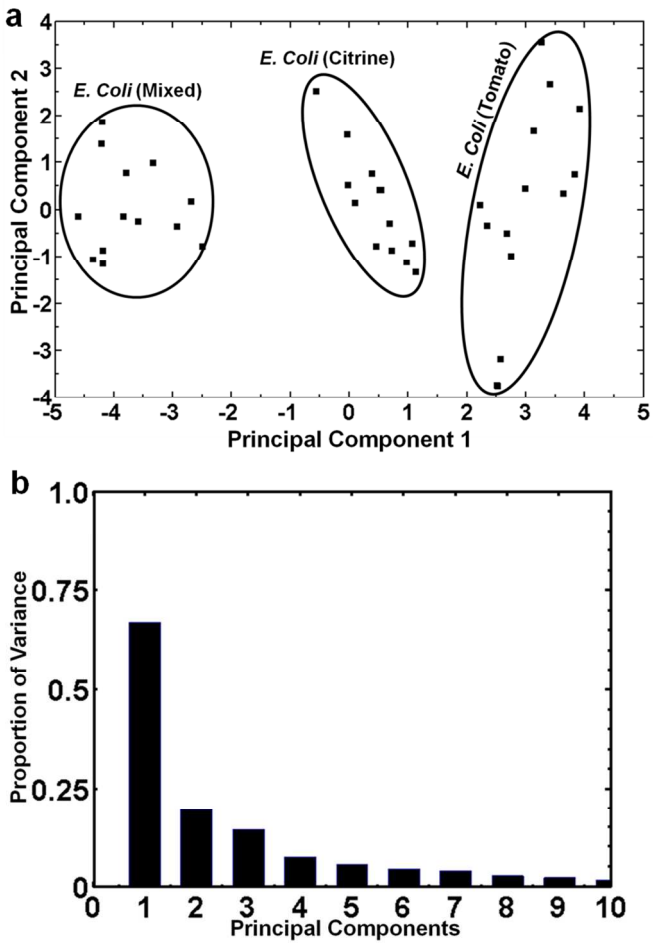

Figure 5: a) Principal component analysis of 7.87 eV laser LDPI-MS of the three different regions of a coculture multistrain *E. coli* (tomato and citrine strains) membrane biofilm. b) Scree plot showing variance of the entire data set with respect to the principal components.

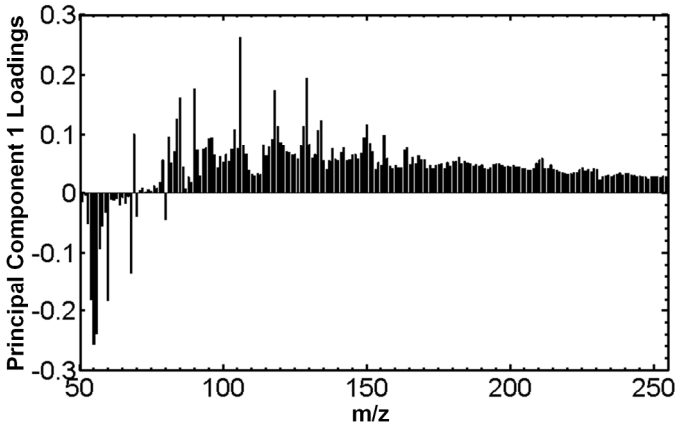

Figure 6: Principal component 1 loadings plot for the entire 7.87 eV laser LDPI-MS data set of the coculture multistrain *E. coli* biofilm.

Figure 6 is the principal component 1 loadings plot, correlating which peaks in the mass spectra are most responsible for the differences seen by PCA between the mixed region and the two "pure" regions of the 7.87 eV laser LDPI-MS. In general, peaks with positive loadings along a given PC axis will show a higher relative intensity in samples with positive scores along the same PC axis (and negative loadings are similarly correlated with negative scores).[12] Figure 5a shows that the *E. coli* mixed region has a negative score while the two pure regions have positive scores along principal component 1. Therefore, negative peaks in Figure 6 loadings plot for PC 1 correspond with the peaks that are more abundant in the mixed region (Figure 5a). Figure 6 and the biplot (not shown) indicate that the mass spectral peaks that contributed the most to the separation of the mixed region from the two pure regions were m/z 55, 56, 60, 68, and 80. Similar analysis of the 7.87 eV data for the two pure regions indicated that peaks at m/z 52, 56, 64, 65, 72, 75, 76, and 78 contributed to the separation of the two strains along the first principal component. PCA of 10.5 eV laser LDPI-MS data indicated that peaks at m/z 54, 63, 64, 66, 79, 81, 86, 88, 94, 138, 152, and 285 contributed to the separation of the two strains. However, it cannot be determined in these experiments which of these peaks are due to parent vs. fragment ions.

PCA was also applied to the synchrotron LDPI-MS data, but no coherent results could be obtained from the analysis. One limitation of the synchrotron LDPI-MS data analysis was simply that too few spectra had been collected for a useful data matrix, a problem to be overcome by further experiments.

IV. Discussion

A. Distinguishing species, strains, and metabolic states by PCA of LDPI-MS data. Different species as well as separate strains and metabolic states of coculture biofilms were distinguished by LDPI-MS detection of endogenous species followed by discrimination of the data by PCA. This is especially remarkable for the multistrain system because the strains differed from the wild type K-12 strain by no more than four gene deletions each out of approximately 2000 genes [8] and the manual examination of the mass spectral data showed barely any difference.[25] PCA treatment of 7.87 eV LDPI-MS data separated the strains into three distinct groups (see Figure 5a): two "pure" groups and a mixed region. Furthermore, the "pure" regions of the cocultures showed greater variance by PCA when analyzed by 7.87 eV photon energies than by 10.5 eV radiation. It is noteworthy that the *E. coli* mixed region (Figure 5a) has a negative score along principal component 1 which results in its grouping outside of the pure tomato and citrine regions. This indicates that the mixed region constitutes a different collective metabolic profile than a simple summation of the pure metabolisms, possibly due to inter-strain interactions via metabolite or quorum sensing-like exchange. LDPI-MS was also able to distinguish the bacteria from the yeast studied here both without and with the application of PCA, both significant accomplishments. Overall, it is clear that LDPI-MS should be considered as another tool in the MS methods available to probe local metabolic states and exchange in microbial systems.[6]

The principal component 1 loadings plot for the 7.87 eV laser LDPI-MS data (Figure 6) revealed several mass spectral peaks which contributed the most to the separation of the strains. For example, the m/z 60 peak showed a higher relative intensity in the mixed region (Figure 6) and contributed to the separation of the mixed region from the "pure" regions. This peak might

have arisen from the molecular ion of acetate, which is known to be in abundance in the mixed region.[8] The principal component 1 loadings plot of the 10.5 eV laser LDPI-MS showed that m/z 285 contributed to the difference between the two *E. coli* strains. M/z 285 could be attributed to the stearic acid parent ion, which is a common constituent of the *E. coli* cell walls and membranes.[25] It can be hypothesized that the two strains' metabolisms create locally different microenvironments that may influence membrane composition.

Both the synchrotron and laser LDPI-MS indicated that different classes of molecules can be targeted with different photon energies. Table 1 shows new peaks appearing with increasing photon energy, as expected since many organic compounds have ionization energies in the 9 - 10 eV range and single photon ionization requires VUV photon energies in excess of a molecule's ionization energy.[22,35] Comparison of the 7.87 and 10.5 eV data is consistent with the expectation that the lower photon energy selects a subset of low ionization energy analytes while 10.5 eV is more inclusive, detecting across a wider range of analytes. These two VUV photon energies therefore give different spreads via PCA and they constitute an additional experimental parameter to differentiate strains and species. Many metabolites have relatively low molecular weights, so their molecular ions will be found in the low mass region. The lower mass region is of particular note in the 7.87 eV LDPI-MS of the *E. coli* cocultures.

Several metabolites were tentatively assigned to the observed MS peaks based on the ability of 7.87 eV photon energy to selectively ionize species containing tertiary amines and fused ring structures.[21] These tentative assignments were made by referring to *E. coli*[36] and yeast[37] metabolite databases. *E. coli* peaks at m/z 102, 104, 114, 138, 140, 143, 145, 157, and 366 were assigned to betaine aldehyde, choline, 2-mercapto-1 methylimidazole, urocanic acid, L-histidinal, crotonobetaine, gamma-butyrobetaine, imidazolelactic acid, and phosphoribosyl

formamidocarboxamide, respectively. Yeast peaks at m/z 157, 240, 243, 244, 252, 267, 284, and 720 were assigned to N-acetyl-D-proline, anserine, cytidine, uridine, 2'-deoxyinosine, adenosine, xanthosine, and phosphoribosyl-ATP, respectively.

Additionally, *E. coli* peaks at m/z 625, 635, 732 and 763 and yeast peaks at m/z 723, 724, 840, and 843 correspond with the molecules in the glycerophospholipids class, an abundant constituent of the microbial cell membrane. These molecules do not have tertiary amines or fused ring moeities in their structure, leading to the speculation that they may have desorbed as clusters which facilitates their VUV postionization.[27]

Additional classes of molecules will be photoionized at 9.5 and 10.5 eV photon energies, increasing the possibility of the parent ions of different endogenous species appearing at the same nominal m/z values. Nonetheless, tentative assignments were made for some 9.5 and 10.5 eV peaks in Table 1. *E.coli* peaks at m/z 153, 228, 240, 256, and 338 could be attributed to to 3-sulfinoalanine, myristic acid, L-cystine, palmitic acid, and N5-carboxyaminoimidazole ribonucleotide, respectively. Peaks at m/z 665, 750 and 775 were assigned to the molecules of glycerophospholipids. Similarly, yeast peaks at m/z 146, 149, 189, 190, 192, 200, 213, and 214 were assigned to L-glutamine, D-methionine, N-acetyl-L-glutamic acid, oxalosuccinic acid, citric acid, lauric acid, 4-phopho-L-aspartic acid, and 3-methylbutyl octanoate, respectively. Peaks at m/z 565, 567 and 593 were assigned to glycerolipids and peaks at m/z 426, 494 and 522 were assigned to glycerophospholipids. Regardless of photon energy, high resolution or tandem MS analysis is required to unequivocally associate any of the aforementioned peaks with specific endogenous species in the cocultures.

B. Comparison of MS imaging methodologies for biofilms. Thick, intact biofilm samples grown on insulating membranes were successfully analyzed using laser LDPI-MS.

Polycarbonate membranes provided a surface for robust growth of coculture biofilms and can produce visually obvious boundaries between different species or strains. However, biofilms grown on membranes were ~0.5 - 1 mm thick and displayed topographical features that can hinder analysis by SIMS and MALDI-MS imaging. Synchroton LDPI-MS was able to successfully analyze blots of biofilms, which can also be analyzed by laser LDPI-MS, SIMS and MALDI-MS.[16] Prior work examined biofilms grown using drip flow reactors,[26] but coculture biofilms grown by drip flow tend to lack clear boundaries between segregated species. Significantly higher laser desorption energy was required to analyze intact membrane biofilms compared to the blotted biofilms. This might have resulted from the thickness of the membrane biofilms and the effective absence of an immediately adjacent metal substrate which otherwise can undergo rapid heating to assist desorption.[29,38]

With its ability to analyze intact biological samples with reasonable spatial resolution, LDPI-MS can be used to study a range for biological samples such as infected medical implants, dental composites, or tooth samples. Spatial resolution here was limited to the mm-scale due to the relatively low signal that required collection of spectra from relatively large areas of the biofilms. Prior work reported a spatial resolution of ~20 μm is achievable with the laser LDPI-MS instrument, but resolution for MS imaging was limited to vibrations and was ~50 μm due to the low repetition rate of the Nd:YAG laser used to pump the 10.5 eV source.[25] Synchrotron LDPI-MS has demonstrated a resolution of better than 5 μm on an organic photoresist structure[29] and recently, 4.2 μm resolution has been achieved on a cross section of poplar wood.

Several studies have been reported which applied PCA to MALDI-MS data to obtain differentiation of species or strains as well as biomarker profiling.[13,14] However, it is noteworthy that the difference in MALDI mass spectra due to ion suppression and matrix peaks could result

in unwanted sample separation during PCA. Furthermore, low molecular weight metabolite analyses by MALDI-MS can be impeded by matrix ion interferences. By contrast, LDPI-MS can analyze the low mass region of coculture biofilms without addition of any interfering matrix or other sample preparation.

SIMS has the advantage of high resolution and high sensitivity in the low mass region, both useful for studying metabolites and other small endogenous species. However, useful information is difficult to obtain for masses over m/z 300, which limits its application to a reduced set of target molecules.[12,15,18,39] The results presented here showed LDPI-MS peaks up to m/z 1000, indicating its potential use for target species with a larger mass range than commonly available to SIMS.

Laser LDPI-MS of intact membrane biofilms showed overall higher signal intensity than from blotted samples. This could be due to the difference in desorption efficiency for the two samples. By contrast, blotting of the biofilm resulted in loss of structural integrity and reduced sample volume that decreased the overall signal intensity.

The data presented here was acquired with two different LDPI-MS instruments. The synchrotron LDPI-MS instrument used tunable VUV for postionization that allowed exploration of the effect of increasing photon energies on mass spectral profiles. The synchrotron LDPI-MS showed overall higher signal intensity and with appropriate sample preparation should allow for high resolution imaging of microbiological systems. Prior work on non-biofilm samples demonstrated the utility of tuning across a wide and continuous range of photon energies.[29,35] The 7.87 and 10.5 eV laser LDPI-MS allowed for in house data analysis and optimization as well as examination of electrically insulating samples such as membrane biofilms.

Acknowledgements

The authors acknowledge the assistance of Anjan Roy in developing the multivariant analysis. This work was supported by the National Institute of Biomedical Imaging and Bioengineering via grant EB006532. MA, TH, SL, and the Advanced Light Source were supported by the Director, Office of Energy Research, Office of Basic Energy Sciences, Chemical Sciences Division of the U.S. Department of Energy under contract No. DE-AC02-05CH11231. The contents of this manuscript are solely the responsibility of the authors and do not necessarily represent the official views of the National Institute of Biomedical Imaging and Bioengineering, the National Institutes of Health, or the Department of Energy.

Supporting Information

The following figures and associate text are provided in the Supporting Information.

Figure S1: 7.87 to 10.5 eV synchrotron LDPI-MS of *E. coli* (tomato) strain blotted monoculture biofilms.

Figure S2: 10.5 eV laser and synchrotron LDPI-MS of blotted monoculture biofilms using two different instruments.

Figure S3: 10.5 eV synchrotron LDPI-MS of different regions of a blotted coculture biofilm.

Figure S4: 7.87 eV laser LDPI-MS of three regions of *E. coli* (tomato strain) and yeast coculture membrane biofilm.

Figure S5: Principal component analysis of 10.5 eV laser LDPI-MS of a *E. coli* (tomato strain) and yeast coculture membrane biofilm.

Figure S6: a) Principal component analysis of 10.5 eV laser LDPI-MS of a coculture tomato and citrine *E. coli* membrane biofilm. b) Scree plot showing the variance of the data with respect to the principal components.

Figure S7: PCA PC1 loadings plot from 10.5 eV laser LDPI-MS data for coculture *E. coli* biofilm analyzed in Figure S6.

References

(1) Bandara, H. M. H. N.; Yau, J. Y. Y.; Watt, R. M.; Jin, L. J.; Samaranayake, L. P. J. Medic. Microbiol. 2009, 58, 1623-1631.

(2) Nobile, C. J.; Schneider, H. A.; Nett, J. E.; Sheppard, D. C.; Filler, S. G.; Andes, D. R.; Mitchell, A. P. Curr. Biol. 2008, 18, 1017-1024.

(3) Brenner, K.; You, L.; Arnold, F. H. Trends Biotechnol. 2008, 26, 483-489.

(4) Carlsson, J. Adv. Dental Res. 1997, 11, 75-80.

(5) Bernstein, H.; Carlson, R. P. Comput. Struct. Biotechnol. J. 2012, 3, e201210017.

(6) Phelan, V. V.; Liu, W. T.; Pogliano, K.; Dorrestein, P. C. Nat. Chem. Biol. 2012, 8, 26-35.

(7) Momeni, B.; Brileya, K. A.; Fields, M. W.; Shou, W. eLife Sciences 2013, 2.

(8) Bernstein, H. C.; Paulson, S. D.; Carlson, R. P. J. Biotechnol. 2012, 157, 159-166.

(9) Otto, M. "Chemometrics: Statistics and Computer Application in Analytical Chemistry"; Wiley-VCH: New York, 2007.

(10) Tyler, B. J.; Rayal, G.; Castner, D. G. Biomater. 2007, 28, 2412-2423.

(11) Shrestha, B.; Patt, J. M.; Vertes, A. Anal. Chem. 2011, 83, 2947-2955.

(12) Graham, D. J.; Castner, D. G. Biointerph. 2012, 7, 49.

(13) Chen, P.; Lu, Y.; Harrington, P. B. Anal. Chem. 2008, 80, 1474-1481.

(14) Qian, J.; Cutler, J. E.; Cole, R. B.; Cai, Y. Anal. Bioanal. Chem. 2008, 392, 439-449.

(15) Tyler, B. J.; Rangaranjan, S.; Möller, J.; Beumer, A.; Arlinghaus, H. F. Appl. Surf. Sci. 2006, 252, 6712-6715.

(16) Watrous, J. D.; Dorrestein, P. C. Nat. Rev. Microbiol. 2011, 9, 683-694.

(17) Blaze M.T., M.; Aydin, B.; Carlson, R. P.; Hanley, L. Analyst 2012, 137, 5018-5025.

(18) Trouillon, R.; Passarelli, M. K.; Wang, J.; Kurczy, M. E.; Ewing, A. G. Anal. Chem. 2012, 85, 522-542.

(19) Vertes, A.; Hitchins, V.; Phillips, K. S. Anal. Chem. 2012, 84, 3858-3866.

(20) Fletcher, J. S.; Vickerman, J. C. Anal. Chem. 2013, 85, 610-639.

(21) Hanley, L.; Zimmermann, R. Anal. Chem. 2009, 81, 4174-4182.

(22) Akhmetov, A.; Moore, J. F.; Gasper, G. L.; Koin, P. J.; Hanley, L. J. Mass Spectrom. 2010, 45, 137-145.

(23) Sabbah, H.; Morrow, A. L.; Pomerantz, A. E.; Zare, R. N. Ener. Fuels 2011, 25, 1597.

(24) Blaze M.T., M.; Akhmetov, A.; Aydin, B.; Edirisinghe, P. D.; Uygur, G.; Hanley, L. Anal. Chem. 2012, 84, 9410-9415.

(25) Bhardwaj, C.; Moore, J. F.; Cui, Y.; Gasper, G. L.; Bernstein, H. C.; Carlson, R. P.; Hanley, L. Anal. Bioanal. Chem. 2012, http://dx.doi.org/10.1007/s00216-012-6454-0.

(26) Gasper, G. L.; Takahashi, L. K.; Zhou, J.; Ahmed, M.; Moore, J. F.; Hanley, L. Anal. Chem. 2010, 82, 7472-7478.

(27) Blaze M.T., M.; Takahashi, L. K.; Zhou, J.; Ahmed, M.; Gasper, G. L.; Pleticha, F. D.; Hanley, L. Anal. Chem. 2011, 83, 4962-4969.

(28) Takahashi, L. K.; Zhou, J.; Wilson, K. R.; Leone, S. R.; Ahmed, M. J. Phys. Chem. A 2009, 113, 4035-4044.

(29) Kostko, O.; Takahashi, L. K.; Ahmed, M. Chem., Asian J. 2011, 6, 3066-3076.

(30) Heimann, P. A.; Koike, M.; Hsu, C. W.; Blank, D.; Yang, X. M.; Suits, A. G.; Lee, Y. T.; Evans, M.; Ng, C. Y.; Flaim, C.; Padmore, H. A. Rev. Sci. Instrum. 1997, 68, 1945-1951.

(31) Cui, Y.; Moore, J. F.; Milasinovic, S.; Liu, Y.; Gordon, R. J.; Hanley, L. Rev. Sci. Instrum. 2012, 83, 093702.

(32) Timmins, É. M.; Howell, S. A.; Alsberg, B. K.; Noble, W. C.; Goodacre, R. J. Clin. Microbiol. 1998, 36, 367-374.

(33) Goodacre, R.; Heald, J. K.; Kell, D. B. FEMS Microbiol. Lett. 1999, 176, 17-24.

(34) Gasper, G. L.; Takahashi, L. K.; Zhou, J.; Ahmed, M.; Moore, J. F.; Hanley, L. Nucl. Instrum. Meth. Phys. Res. A 2011, 649, 222-224.

(35) Takahashi, L. K.; Zhou, J.; Kostko, O.; Golan, A.; Leone, S. R.; Ahmed, M. J. Phys. Chem. A 2011, 115, 3279-3290.

(36) Guo, A. C.; Jewison, T.; Wilson, M.; Liu, Y.; Knox, C.; Djoumbou, Y.; Lo, P.; Mandal, R.; Krishnamurthy, R.; Wishart, D. S. Nucl. Acids Res. 2013, 41, D625-D630.

(37) Jewison, T.; Neveu, V.; Lee, J.; Knox, C.; Liu, P.; Mandal, R.; Murthy, R. K.; Sinelnikov, I.; Guo, A. C.; Wilson, M.; Djoumbou, Y.; Wishart, D. S. Nucl. Acids Res. 2012, 40, D815-D820.

(38) Hanley, L.; Kornienko, O.; Ada, E. T.; Fuoco, E.; Trevor, J. L. J. Mass Spectrom. 1999, 34, 705-723.

(39) Cillero-Pastor, B.; Eijkel, G.; Kiss, A.; Blanco, F. J.; Heeren, R. M. A. Anal. Chem. 2012, 84, 8909-8916.

Supporting Information for

Differentiation of Microbial Species and Strains in Coculture Biofilms by Multivariate Analysis of Laser Desorption Postionization Mass Spectra

Chhavi Bhardwaj[1], Yang Cui[1], Theresa Hofstetter[2], Suet Yi Liu[2], Hans C. Bernstein[3], Ross P. Carlson[3], Musahid Ahmed[2] and Luke Hanley[1]

[1]Department of Chemistry, University of Illinois at Chicago, Chicago, IL 60607-7061

[2]Chemical Sciences Division, Lawrence Berkeley National Laboratory, Berkeley, CA 94720

[3]Center for Biofilm Engineering, Montana State University, Bozeman, MT 59717

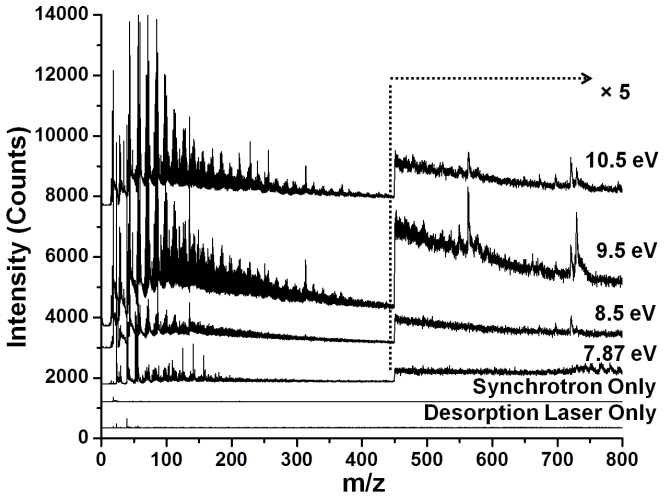

Figure S1: 7.87 to 10.5 eV synchrotron LDPI-MS of *E. coli* (tomato) strain blotted monoculture biofilm. Bottom two traces show the controls performed to check for any background signal.

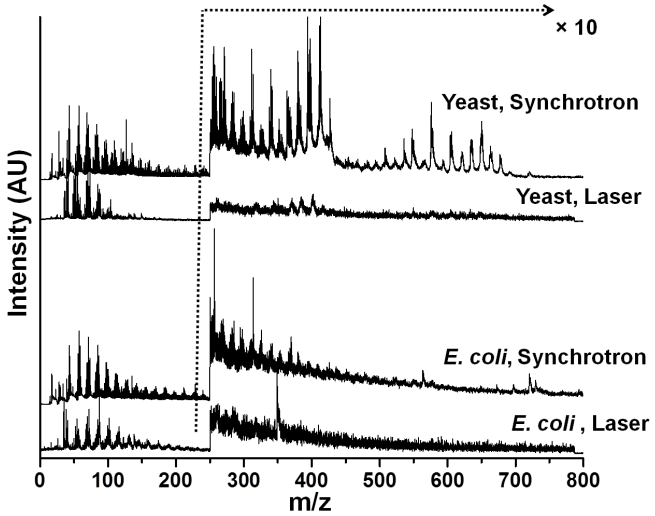

Figure S2: 10.5 eV laser and synchrotron LDPI-MS of blotted monoculture biofilms using two different instruments. *E. coli* (tomato strain) and yeast biofilms. Each spectrum in the figure is normalized to correct for differences in data acquisition strategies between the two instruments.

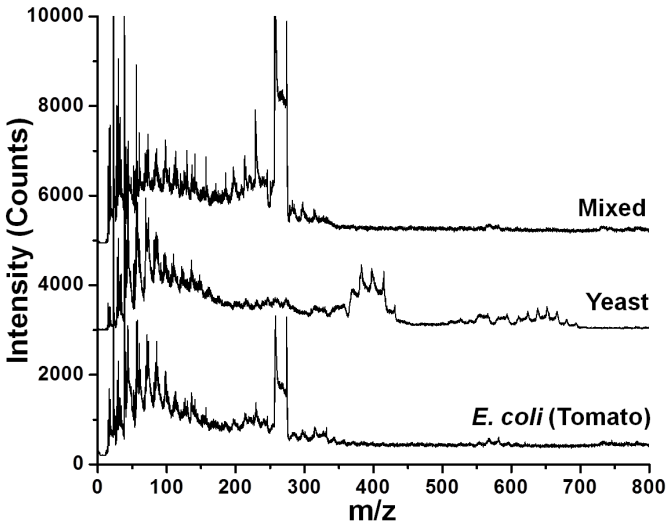

Figure S3: 10.5 eV synchrotron LDPI-MS of different regions of a blotted coculture biofilm. The distinct *E. coli* (tomato strain) and yeast regions as well as the "Mixed" overlapping region were examined.

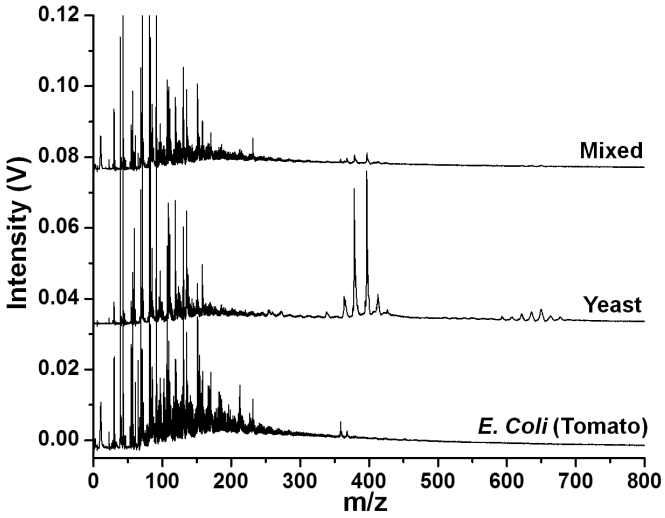

Figure S4: 7.87 eV laser LDPI-MS of three regions of *E. coli* (tomato strain) and yeast coculture membrane biofilm, including the "Mixed" overlapping region.

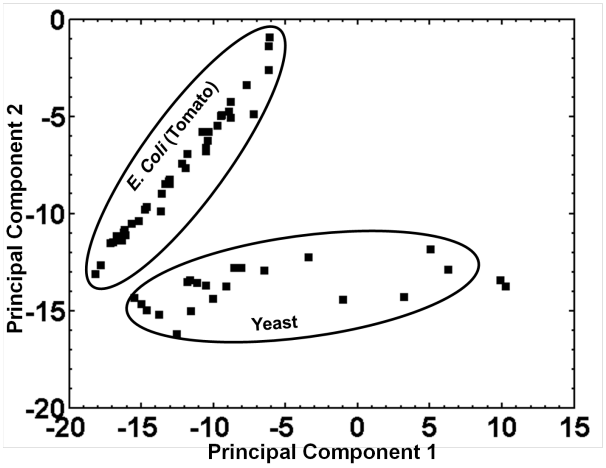

Figure S5: Principal component analysis of 10.5 eV laser LDPI-MS of a *E. coli* (tomato strain) and yeast coculture membrane biofilm, compared the regions of each biofilm that were far from the mixed region that defines the boundary between the two (referred to as "pure" in text).

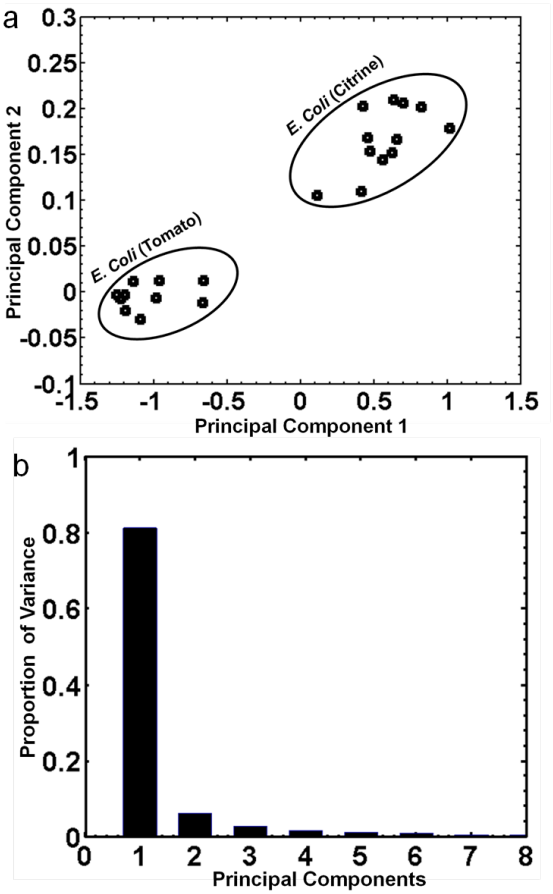

Figure S6: a) Principal component analysis of 10.5 eV laser LDPI-MS of a coculture tomato and citrine *E. coli* membrane biofilm. b) Scree plot showing the variance of the data with respect to the principal components.

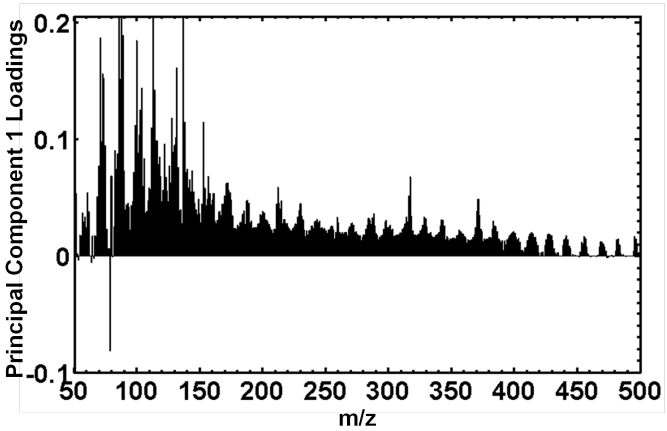

Figure S7: Principle component 1 loadings plot from 10.5 eV laser LDPI-MS data for coculture *E. coli* biofilm analyzed in Figure S6.